BMC Cell Biology

BioMed Central

Research article

GSK-3 inhibitors induce chromosome instability

Anthony Tighe[1], Arpita Ray-Sinha[1,2], Oliver D Staples[1,3] and Stephen S Taylor*[1]

Address: [1]Faculty of Life Sciences, Michael Smith Building, Oxford Road, University of Manchester, Manchester M13 9PT, UK, [2]Division of Surgery and Oncology, University of Liverpool, 5th Floor UCD Building, Daulby Street, Liverpool, L69 3GA, UK and [3]Department of Surgery and Molecular Oncology, Ninewells Hospital, University of Dundee, Dundee DD1 9SY, UK

Email: Anthony Tighe - anthony.tighe@manchester.ac.uk; Arpita Ray-Sinha - arpitaray@hotmail.com; Oliver D Staples - O.D.Staples@dundee.ac.uk; Stephen S Taylor* - stephen.taylor@manchester.ac.uk

* Corresponding author

Published: 14 August 2007

BMC Cell Biology 2007, **8**:34 doi:10.1186/1471-2121-8-34

Received: 2 February 2007
Accepted: 14 August 2007

This article is available from: http://www.biomedcentral.com/1471-2121/8/34

Abstract

Background: Several mechanisms operate during mitosis to ensure accurate chromosome segregation. However, during tumour evolution these mechanisms go awry resulting in chromosome instability. While several lines of evidence suggest that mutations in *adenomatous polyposis coli* (*APC*) may promote chromosome instability, at least in colon cancer, the underlying mechanisms remain unclear. Here, we turn our attention to GSK-3 – a protein kinase, which in concert with APC, targets β-catenin for proteolysis – and ask whether GSK-3 is required for accurate chromosome segregation.

Results: To probe the role of GSK-3 in mitosis, we inhibited GSK-3 kinase activity in cells using a panel of small molecule inhibitors, including SB-415286, AR-A014418, 1-Azakenpaullone and CHIR99021. Analysis of synchronised HeLa cells shows that GSK-3 inhibitors do not prevent G1/S progression or cell division. They do, however, significantly delay mitotic exit, largely because inhibitor-treated cells have difficulty aligning all their chromosomes. Although bipolar spindles form and the majority of chromosomes biorient, one or more chromosomes often remain mono-oriented near the spindle poles. Despite a prolonged mitotic delay, anaphase frequently initiates without the last chromosome aligning, resulting in chromosome non-disjunction. To rule out the possibility of "off-target" effects, we also used RNA interference to selectively repress GSK-3β. Cells deficient for GSK-3β exhibit a similar chromosome alignment defect, with chromosomes clustered near the spindle poles. GSK-3β repression also results in cells accumulating micronuclei, a hallmark of chromosome missegregation.

Conclusion: Thus, not only do our observations indicate a role for GSK-3 in accurate chromosome segregation, but they also raise the possibility that, if used as therapeutic agents, GSK-3 inhibitors may induce unwanted side effects by inducing chromosome instability.

Background

Genome stability requires that the replicated chromosomes are accurately segregated during mitosis [1]. Chromosome segregation is mediated by a microtubule spindle, to which chromosomes attach via their kinetochores, complex microtubule-binding structures which

assemble at the centromeric heterochromatin [2-4]. Kinetochores not only attach chromosomes to the spindle, they also perform two key functions which maintain chromosome stability. Firstly, by undergoing rounds of microtubule capture-and-release, kinetochores select microtubule attachments which yield tension across the centromere [5]. This in turn promotes chromosome biorientation, i.e. sister kinetochores attached to opposite spindle poles. Secondly, by monitoring microtubule occupancy and/or tension, kinetochores regulate the spindle checkpoint, a surveillance mechanism which delays anaphase until all the chromosomes are bioriented [6].

As a consequence of these mechanisms, most normal proliferating human cells are diploid and karyotypically stable. By contrast, many tumour cells exhibit chromosome instability and are therefore karyotypically unstable and aneuploid [7]. Much effort has gone into defining the genetic lesions responsible for the chromosome instability and recently, *adenomatous polyposis coli* (*APC*) has emerged as a candidate, at least in colon cancer [8,9]. APC is best known for its role in the Wnt signalling pathway: in the absence of Wnt signals, a destruction complex of APC and axin recruits both β-catenin and GSK-3 [10,11]. Phosphorylation of β-catenin by GSK-3β then targets β-catenin for proteolysis. In the presence of Wnt signals, β-catenin phosphorylation is inhibited, resulting in the upregulation of proliferative genes. This mechanism is essential for tumour suppressor function in the colonic epithelia: almost all colon cancers have either loss of function mutations in APC or activating mutations in β-catenin [12]. However, APC is a large multi-domain protein and its function is not restricted to the Wnt pathway.

Evidence is mounting that APC is somehow required for the fidelity of chromosome segregation. APC is a microtubule binding protein and has the ability to stabilise plus ends [13]. In mitosis, APC localises to kinetochores in a microtubule dependent manner [14,15], and tumour cells with APC mutations have weaker kinetochore – microtubule interactions [16,17]. Spindles assembled in *Xenopus* egg extracts depleted of APC are abnormal [18]. APC also localises to centrosomes [19-21], and in the *Drosophila* germ line, APC is required for spindle positioning [22]. In mice, APC mutation enhances genomic instability and tumour formation in cells haploinsufficient for BubR1, a spindle checkpoint kinase [23]. Murine embryonic stem cells with APC mutations are frequently tetraploid [14,15]. Ectopic expression of N-terminal APC mutants in diploid, APC-proficient human cells compromises the spindle checkpoint and enhances survival following prolonged mitotic arrest, leading to aneuploidy [21]. However, despite this body of evidence, the molecular mechanisms linking APC and chromosome instability remain unclear.

One possibility is that APC mutation compromises EB1, a microtubule tip-tracking protein involved in microtubule dynamics, spindle positioning, chromosome stability and cytokinesis [24,25]. EB1 binds the C-terminus of APC [26], so it is conceivable that the binding of N-terminal APC mutants to partners, including full length APC, excludes EB1 from complexes required for microtubule processes [17]. Another possible mechanism lies with, GSK-3. Like APC, the function of GSK-3 is not restricted to the Wnt pathway, rather it has been implicated in a plethora of processes including glycogen metabolism and tau phosphorylation [27-29], and more recently, regulating kinesin-driven organelle movement [30] and Cyclin E degradation [31]. Importantly, GSK-3 has been implicated in regulating interphase microtubule dynamics [32]. Phosphorylated GSK-3 localises to spindle poles in mitosis [33]. In both budding and fission yeast, overexpression of GSK-3 suppresses mutations in kinetochore proteins and the centromeric DNA [34,35]. Interestingly, Bub1 and BubR1, two related protein kinases which localise to kinetochores and are required for spindle checkpoint function [36], phosphorylate APC *in vitro* [15]. While the significance of this is unclear, phosphorylation is enhanced if APC is already phosphorylated by GSK-3 [15]. In one study, small molecule GSK-3 inhibitors were shown to induce spindle defects and chromosome misalignment [33]. However, whether these chromosomes eventually aligned before anaphase onset is unclear. Indeed, we envision two possible scenarios; either the chromosomes never align, yielding prolonged checkpoint arrest followed by adaptation and mitotic exit without dividing, yielding tetraploid cells [37]; or alternatively, the spindle checkpoint "gives up" and the cells enter anaphase despite unaligned chromosomes, thereby missegregating only those chromosomes [38].

To distinguish between these possibilities and further probe the role of GSK-3 in mitotic chromosome segregation, we characterised a panel of structurally diverse GSK-3 inhibitors. We show that these inhibitors have profound effects on cell cycle control, spindle morphology and chromosome alignment. Strikingly, these inhibitors increase the frequency with which cells missegregate their chromosomes. In support of the notion that these phenotypes are due to inhibition of GSK-3, rather than off target effects, we use RNA interference to selectively repress GSK-3β. This results in a chromosome alignment defect and the formation of micronuclei, a hallmark of chromosome missegregation.

Results

Characterisation of small molecule GSK-3 inhibitors

A number of small molecules have been identified which inhibit GSK-3 *in vitro* [27]. To determine whether GSK-3 is required for accurate chromosome segregation, we

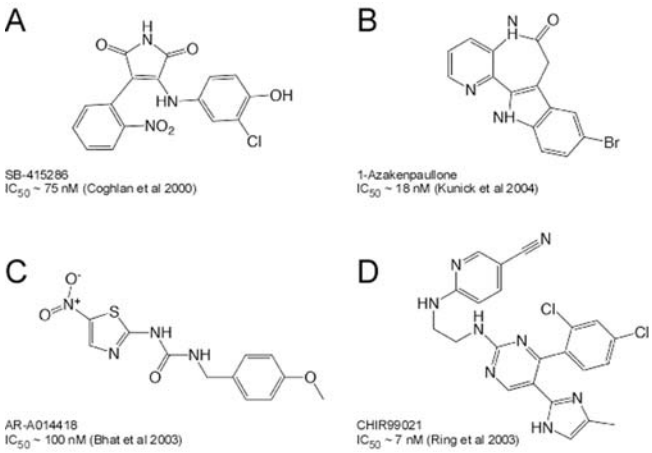

Figure 1
Small molecule inhibitors of GSK-3. Chemical structures of SB-415286, 1-Azakenpaullone, AR-A014418 and CHIR99021

obtained a panel of structurally diverse inhibitors (Fig. 1 and Table 1) and tested their ability to inhibit glycogen synthase (GS) phosphorylation in cells [39,40]. As a negative control, we used DMSO, the solvent in which the drugs were dissolved, and as a positive control we used lithium chloride, a well established GSK-3 inhibitor [41,42]. When HeLa cells were treated with GSK-3 inhibitors for 24 hours, only SB-415286, AR-A014418, 1-Azakenpaullone, CHIR99021 and Inhibitor XI significantly reduced GS phosphorylation (Fig. 2A). TDZD-8, Inhibitor II and OTDZT had little effect (Fig. 2A), even when used at relatively high concentrations (not shown).

Several GSK-3 inhibitors have been shown to inhibit members of the CDK family, at least in vitro [27]. We therefore asked whether cellular Cdk1 activity was inhibited by the GSK-3 inhibitors used here. HeLa cells were synchronised in mitosis with nocodazole then exposed to GSK-3 inhibitors. In parallel, cells were exposed to a bone fide Cdk1 inhibitor, RO-31-8220 [43]. To prevent mitotic exit, the proteasome inhibitor MG132 was also added to the cells. Cell lysates were then prepared and immunoblotted for phospho-nucleolin, a known Cdk1 substrate (Fig. 2B). While RO-31-8220 clearly inhibited the phosphorylation of nucleolin, the GSK-3 inhibitors had no apparent effect. Thus, at the concentrations where GSK-3 is clearly inhibited (Fig. 2A), there does not appear to be any appreciable inhibition of Cdk1.

Next, we analysed spindle morphology in drug-treated mitotic DLD-1 cells. In controls, or cells treated with compounds which did not inhibit GS phosphorylation, normal metaphase spindles were readily apparent (Fig. 2C). By contrast, cells treated with compounds which did inhibit GS phosphorylation, frequently exhibited abnormal chromosome configurations. Specifically, although bipolar spindles formed and most chromosomes aligned at the metaphase plate, some chromosomes were often clustered near the spindle poles (Fig. 2C). For example, in the presence of the highly specific GSK-3 inhibitor, CHIR99021, ~49% of metaphases had one or more chromosomes clustered near the spindle poles (Fig. 2D). Thus, five structurally diverse small molecules which inhibit GSK-3 activity in cells induced a chromosome alignment defect.

GSK-3 inhibitors delay mitotic entry and exit

Although GSK-3 inhibitors have been used extensively to study insulin action [44-47], very little is know about their effects on the cell cycle. In light of the observation described above, we therefore analysed the effect of GSK-3 inhibitors on cell cycle progression. HeLa cells were synchronised in early S-phase using a double thymidine block then released into drug free media, or media supplemented with SB-415286 or nocodazole. Over the next 24 hours cells were harvested at regular intervals and analysed by flow cytometry to determine DNA content and mitotic index. Control cells progressed through S-phase then entered mitosis 9 hours after release (Fig. 3A, B). The mitotic index peaked at ~20% 10 hours post-release then, as division was completed, cells with 2N DNA contents reappeared. 17 hours post-release, i.e. 5–6 hours after returning to G1, these cells entered a second S-phase. Cells

Table 1: GSK-3 inhibitors used in this study

Compound	Class	Mechanism	In vitro IC_{50}	Conc. used in cells	Ref.
SB-415286	Arylindole-maleimides	ATP Competitor	78 nM	30 μM	[44]
AR-A014418	Thiazole	ATP Competitor	104 nM	20 μM	[58]
1-Aza kenpaullone	Benzazepinone	ATP Competitor	18 nM	2.5 μM	[57]
CHIR99021	Aminopyrimidine	ATP Competitor	7 nM	10 μM	[47]
Lithium	Divalent ion	Non competitive	2 mM	40 mM	[41]
TDZD-8	Thiadiazolidinone	Non competitive	2 μM	10–60 μM	[70]
Inhibitor II	Pyridyloxadiazole	-	390 nM	25–75 μM	[71]
OTDZT	Thiadiazolidinone	Non competitive	10 μM	50–100 μM	[70]
Inhibitor XI	Azaindolylmaleimide	ATP Competitor	32 nM	50 μM	[72]

Table 2: Effect of SB-415286 inhibitors on mitotic timing

Compound	Event	Time (mins)	s.e.m.	Range	N	P
Untreated	NEB-Metaphase	21.59	1.49	12–72	41	-
	Metaphase-Anaphase	10.65	0.92	1.5–35.5	49	-
SB-415286	NEB-Metaphase	46.04	4.32	17.5–162	42	$p < 0.01$
	Metaphase-Anaphase	11.32	1.2	1.5–55	57	$p > 0.05$

Values represent the mean time, in minutes, taken from nuclear envelope breakdown to metaphase and metaphase to anaphase in minutes. Also shown is showing the standard error of the mean, the range and the number of cells analysed. P values determined using a Kruskal-Wallis test.

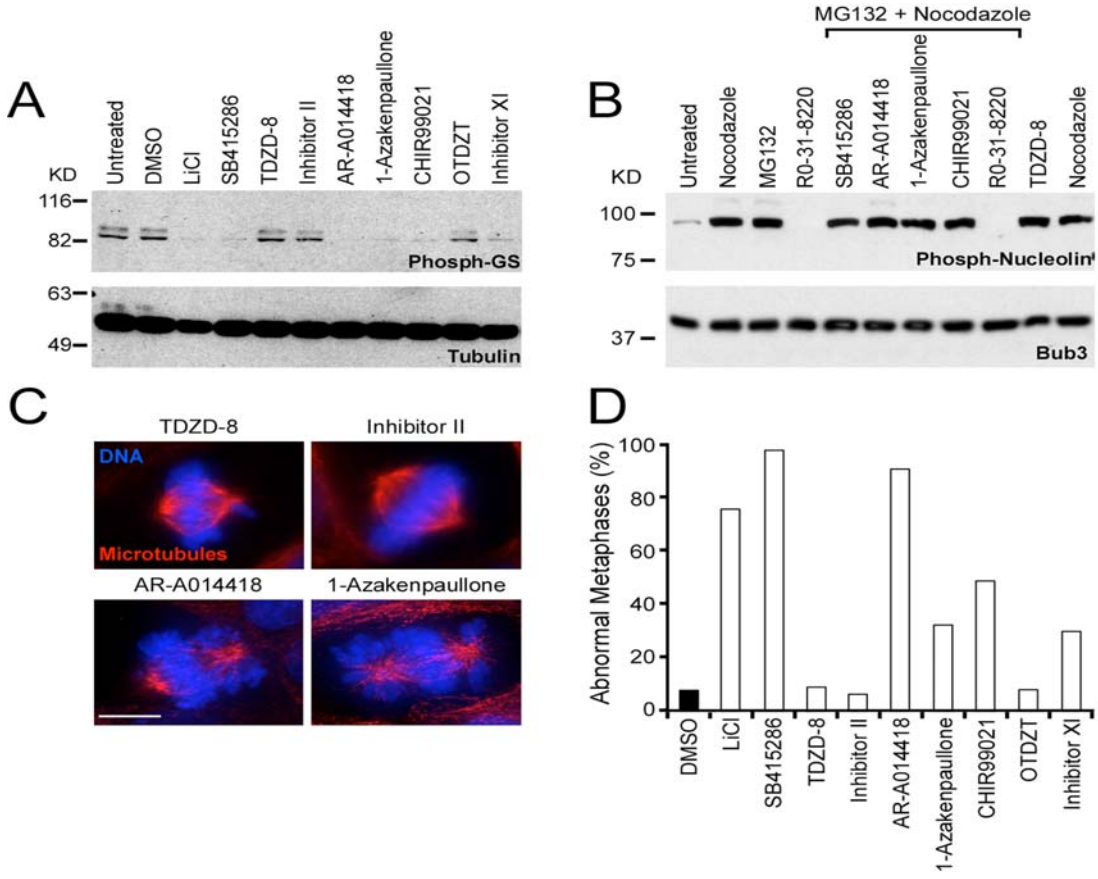

Figure 2

Identification of small molecules which inhibit GSK-3 *in vivo*. HeLa and DLD-1 cells were incubated with small molecule GSK-3 inhibitors for 24 hours then analysed by immunoblotting and immunofluorescence. (**A**) Immunoblot of HeLa cell extracts showing inhibition of glycogen synthase phosphorylation by a subset of GSK-3 inhibitors. (B) Immunoblot of HeLa cell extracts showing that GSK-3 inhibitors do not inhibit Cdk1 phosphorylation of nucleolin. (**C**) Images of mitotic DLD-1 cells showing examples of abnormal metaphase spindles following exposure to AR-A014418 and 1-Azakenpaullone. (**D**) Bar graph plotting the number of abnormal metaphases in cells treated with different small molecule GSK-3 inhibitors.

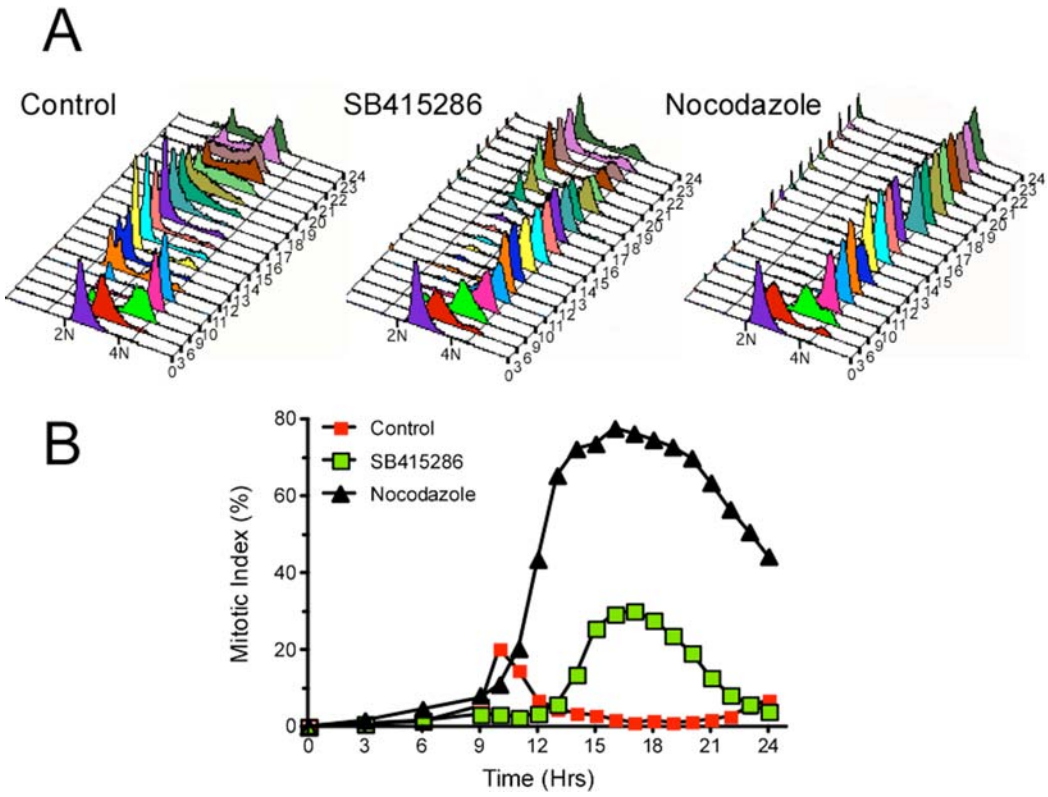

Figure 3
GSK-3 inhibitors delay mitotic entry and exit. HeLa cells were synchronised at G1/S then released into drug-free medium or medium containing either SB-415286 or nocodazole. At the time points indicated the cells, were harvested and analysed by flow cytometry to determine DNA content and mitotic index. (**A**) DNA content histograms showing that SB-415286 delays cell division. (**B**) Graph plotting the mitotic index, as determined by MPM-2 reactivity, showing that mitotic progression is delayed in SB-415286 treated cells.

released into nocodazole completed S-phase but then, consistent with hyper-activation of the spindle checkpoint, arrested in mitosis maintaining 4N DNA contents. Cells released into SB-415286 also progressed through the first S-phase will normal kinetics (Fig. 3A) but the mitotic index did not increase until 13 hours post-release, indicating a mitotic entry delay of ~3 hours (Fig. 3B). 17 hours post-release, the mitotic index peaked at ~30%. After this, the number of cells with 2N DNA contents started to increase, indicating successful cell division. By 23 hours, i.e. ~6 hours after they returned to G1, SB-415286-treated cells entered a second S phase. Thus in HeLa cells, SB-415286 has no apparent effect on G1/S progression and neither does it prevent cell division. SB-415286 does however delay mitotic entry and mitotic exit.

GSK-3 inhibitors delay chromosome alignment

To determine why SB-415286 delayed mitotic progression, we analysed drug-treated DLD-1 cells by time-lapse microscopy, using a GFP-tagged histone to visualise the chromosomes [38]. Control cells typically aligned their chromosomes within ~22 minutes (Table 2) then underwent a normal anaphase (Fig. 4A). Note that untreated cells never entered anaphase with unaligned chromosomes (Table 3). By contrast, chromosome alignment was often delayed in SB-415286 treated cells and anaphase was often initiated with unaligned chromosomes. For example, Figure 4B shows two cells, marked ***a*** and ***b***, which, at T = 34 minutes still have unaligned chromosomes (one in ***a***, and two in ***b***, see arrow head and arrows respectively). At T = 39 minutes, the last chromosome in cell ***a*** aligns and anaphase initiates at T = 46. By T = 96.5 minutes, one of the laggards in cell ***b*** has congressed, but

Table 3: Effect of GSK-3 inhibitors on mitotic timing and chromosome non-disjunction

Compound	Time (mins)	s.e.m.	Range	N	#	P
-	25.37	0.35	16–42	189	0	-
SB4	69.56	3.44	26–214	99	15	$p < 0.001$
AR	92.88	10.02	24–268	41	3	$p < 0.001$
Ken	31.87	0.48	20–82	348	2	$p < 0.001$
CHIR	43.94	1.93	20–214	187	8	$p < 0.001$

Values represent the mean time, in minutes, taken from nuclear envelope breakdown to metaphase, Also shown is the standard error of the mean, the range, the number of cells analysed (N), the number of cells which enter anaphase with unaligned chromosomes (#). P values determined using a Kruskal-Wallis test.

one remains unaligned (see asterisk). At T = 100.5, cell ***b*** enters anaphase, without the last chromosome aligning.

To quantitate these effects, we measured the time taken from prophase to metaphase, i.e. when the last chromosome aligned, and the time taken from metaphase to anaphase. While control cells took 21.6 ± 1.4 minutes to reach metaphase, SB4-treated cells took, on average, 46.0 ± 4.3 minutes (Fig. 4C, Table 2). Anaphase initiated ~11 minutes later in both control (10.7 ± 0.9 minutes) and SB-415286-treated (11.3 ± 1.2 minutes) cells. Importantly however, six out of thirty-two SB-415286 treated cells entered anaphase with one or more unaligned chromosomes. This phenomenon was not restricted to SB-415286. In a separate set of experiments, we measured the time from nuclear envelope breakdown (NEB) to anaphase in the presence of SB-415286, AR-A014418, 1-Azakenpaullone and CHIR99021. Like SB-415286, AR-A014418 induced a prolonged mitotic delay (NEB to anaphase, 92.9 ± 4 minutes, Fig. 4D, Table 3). Following chromosome alignment, anaphase initiated with normal kinetics (not shown), confirming that the prolonged mitosis was due to delayed chromosome alignment. 1-Azakenpaullone and CHIR99021 induced modest but never-the-less significant ($p < 0.001$) delays, (Fig. 4D, Table 3). Importantly, a proportion of the cells exposed to AR-A014418, 1-Azakenpaullone and CHIR99021 entered anaphase with unaligned chromosomes (Table 3).

To see if such chromosome missegregation events would lead to aneuploidy, diploid HCT116 cells were exposed SB-415286 for 48 hours, metaphase spreads prepared then chromosome number determined. At day 0, the majority of untreated control cells had a near diploid karyotype, with only 3% of the cells having more than 49 chromosomes (not shown). By contrast, 13.4% of cells treated with SB-415286 had more than 49 chromosomes. By day 5, the aneuploid population (>49 chromosomes) in control cells was 5.6%, however in SB-415286 treated cells, 26.3% were now aneuploid (not shown).

Thus, when exposed to GSK-3 inhibitors, chromosome alignment is delayed and anaphase is often initiated in the presence of unaligned chromosomes yielding aneuploid cells.

GSK-3 inhibitors induce mono-orientations

To determine why complete chromosome alignment was delayed in cells treated with GSK-3 inhibitors, we analysed K-fibres using high-resolution optical sectioning microscopy. To visualise centromeres and kinetochores, we stained cells with anti-centromere antibodies (ACA) and anti-BubR1 antibodies respectively. In control cells, chromosomes near the spindle equator were clearly bioriented: microtubules terminated at BubR1 foci which were connected by ACA staining (Fig. 5A). In drug-treated cells, chromosomes near the spindle equator also appeared to be correctly bioriented (Fig. 5B). However, chromosomes near the spindle poles were typically mono-oriented, with one kinetochore attached to the nearest spindle pole and the other unattached (Panels ***i*** in Fig. 5D, E). In some cases, microtubules from the same pole could be seen extending towards both kinetochores of an unaligned chromosome, indicating a possible syntelic orientation (Fig. 5C and panels ***ii*** in 5D, E). Thus, while GSK-3 inhibitors do not prevent kinetochore biorientation or chromosome congression, they do appear to inhibit the ability of a cell to perfectly biorient all its chromosomes.

GSK-3 inhibitors alter spindle morphology

During the analysis described above (Figs 2B and 5), we noticed that in drug-treated cells, spindle morphology appeared abnormal in that there appeared to be increased astral microtubules near the pole around which chromosomes clustered. In addition, spindle length appeared to increase. Examples of both these phenotypes are shown in Figure 6A. In panel ***i***, the control cell shows a normal spindle morphology, with the chromosomes aligned between two robust crescent-shaped half spindles, and a small number of astral microtubules projecting away from the poles. In panel ***ii***, the spindle seems abnormally long, with the half spindles forming cones rather than crescents. In panel ***iii***, the pole on the right appears as a radial aster

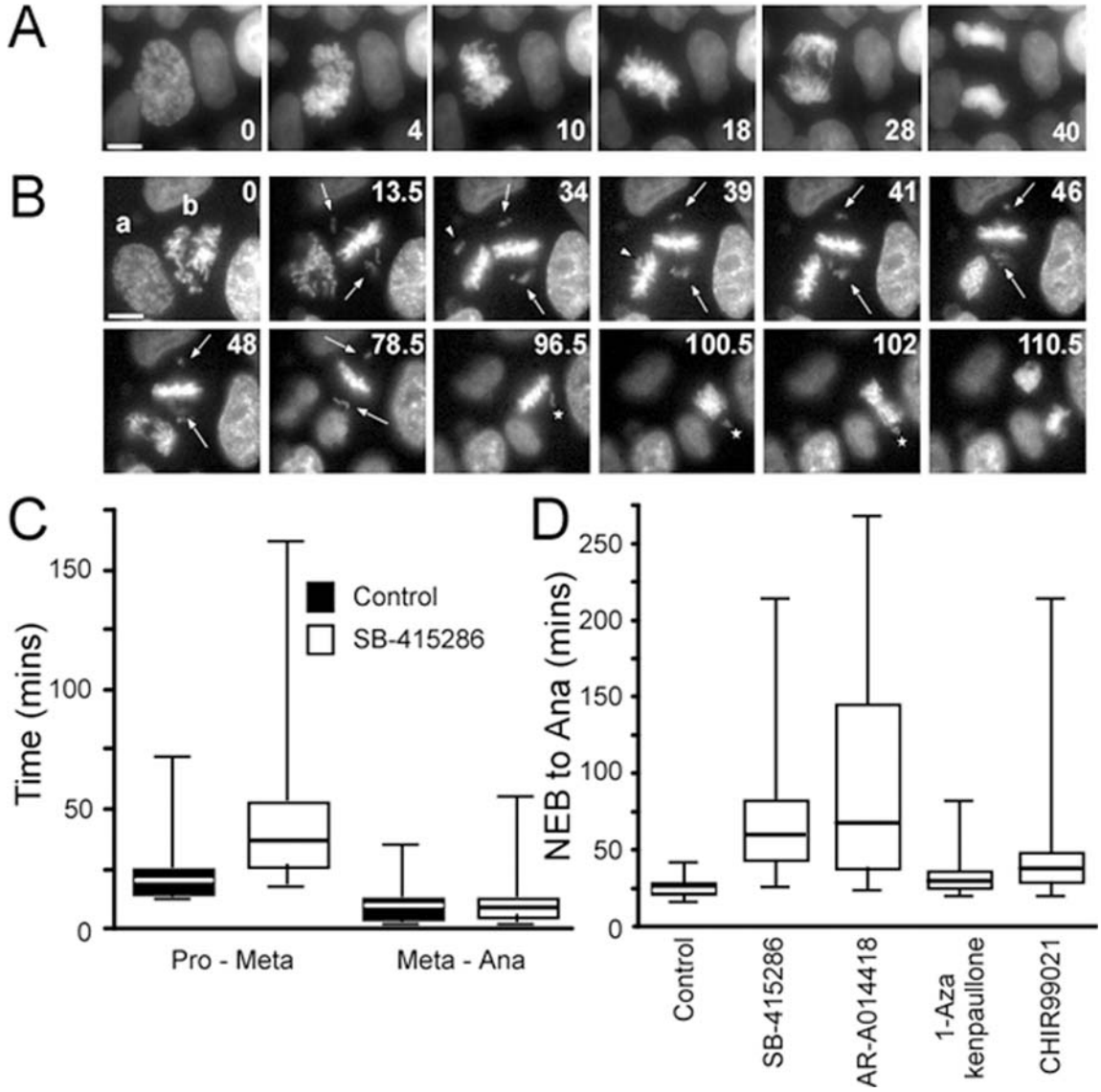

Figure 4

GSK-3 inhibitors delay chromosome alignment. DLD-1 cells expressing a tagged GFP-Histone H2B were incubated in the presence or absence of small molecule GSK-3 inhibitors then analysed by time-lapse microscopy. (**A**) Control cell showing normal mitosis. (**B**) SB-415286-treated cells. While cell ***a*** completes mitosis normally, chromosome alignment in cell ***b*** is delayed (see arrows) and anaphase is initiated despite one unaligned chromosome (see *). (**C**) Box plot measuring time from prophase to metaphase and metaphase to anaphase for at least 42 cells. (**D**) Box plot measuring time taken from nuclear envelope breakdown (NEB) to anaphase onset. Values taken from at least 41 cells.

with equal numbers of microtubules pointing in all directions, rather than a crescent oriented towards the spindle equator.

To quantitate these differences, we measured tubulin fluorescence intensities from one end of the cell to the other along the spindle axis [48]. When plotted as a function of spindle position, the tubulin intensity typically gave two peaks, corresponding to the spindle poles, and a trough,

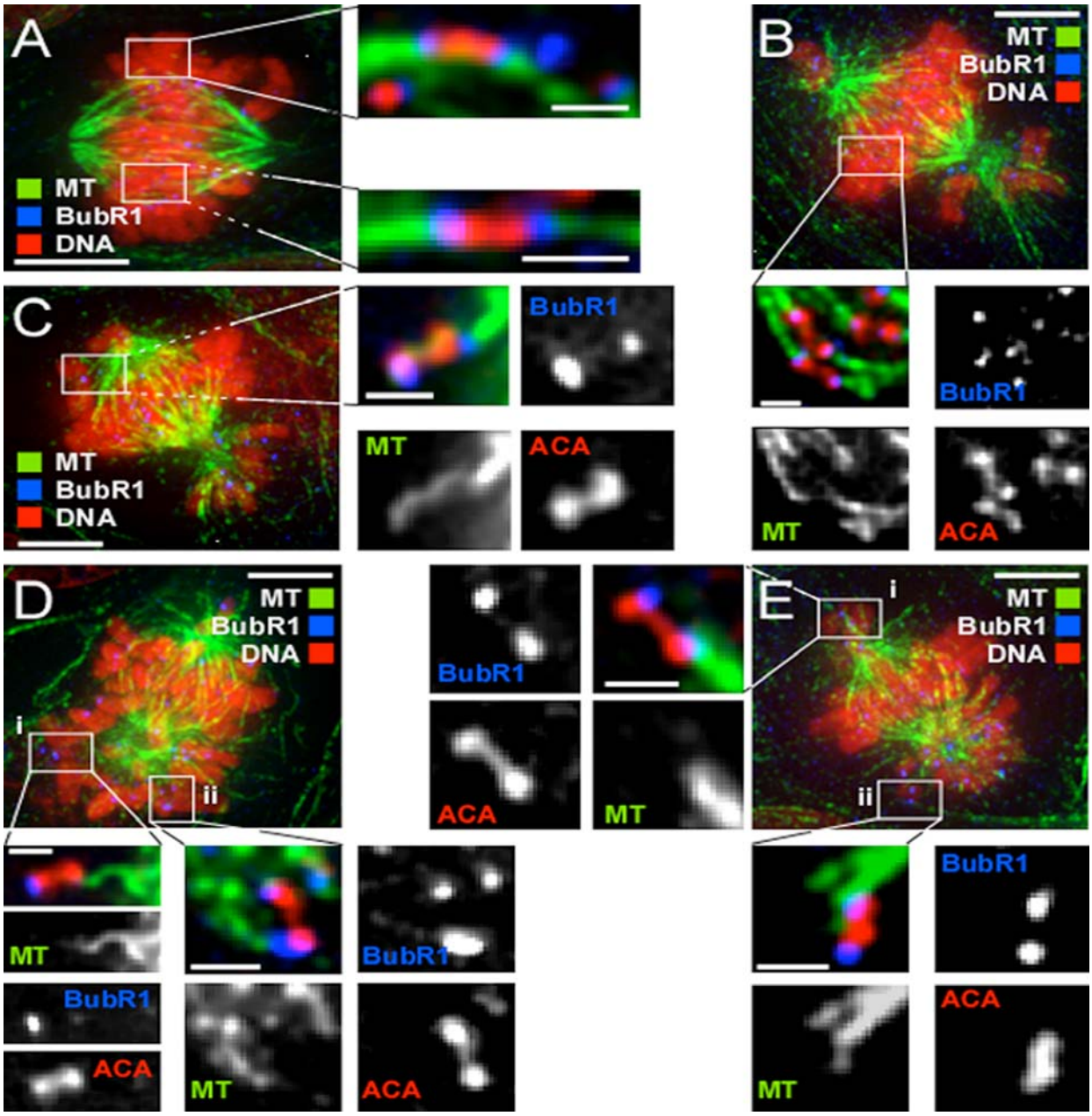

Figure 5

GSK-3 inhibitors yield monopolar and syntelic attachments. DLD-1 cells were incubated with GSK-3 inhibitors for 24 hours then fixed and stained to detect DNA (red), tubulin (green), BubR1 (blue) and centromeres (ACA, red) as indicated. Images represent projections of deconvolved image stacks. (**A**) Control cell showing examples of bioriented chromosomes. (**B**) GSK-3 inhibitor treated cell showing that chromosomes near the metaphase plate are bioriented. (**C-E**) Inhibitor treated cells showing examples of either syntelic attachments (C, Dii, Eii) or monopolar attachments (Di, Ei). Bar is 5 μm when the entire spindle is shown or 1 μm in the enlargements. The cells in C-E were treated with 30 μM SB-415286.

Table 4: Effect of GSK-3 inhibitors on spindle morphology

Parameter	Control	SB-415286	AR-A014418	1-Aza kenpaullone	CHIR99021
Pole-Pole Distance (μm)	8.39 ± 0.45	9.45 ± 0.37	10.36 ± 0.57	9.06 ± 0.39	8.18 ± 0.33
	(22)*	(20)	(19)	(20)	(18)
	-	p > 0.05§	p < 0.05	p > 0.05	p > 0.05
Tubulin Intensity (midzone/cell max)	0.39 ± 0.02	0.21 ± 0.01	0.25 ± 0.01	0.24 ± 0.01	0.26 ± 0.02
	(15)*	(20)	(19)	(20)	(18)
	-	p < 0.001	p < 0.01	p < 0.001	p < 0.05
Interkinetochore Distance (μm)	0.91 ± 0.04	1.04 ± 0.03	1.05 ± 0.04	0.93 ± 0.02	0.92 ± 0.02
	(40, 4)	(33, 4)	(20, 3)	(52, 4)	(41, 4)
	-	p < 0.05	p > 0.05	p > 0.05	p > 0.05
Bub1 Intensity (Bub1:ACA)	100.00 ± 3.30	42.59 ± 0.85	24.24 ± 0.40	46.20 ± 0.98	68.50 ± 0.79
	(76, 4)‡	(64, 4)	(116, 3)	(81, 4)	(124, 5)
	-	p < 0.05	p < 0.001	p < 0.001	p > 0.05
BubR1 Intensity (BubR1:ACA)	100.00 ± 0.40	63.67 ± 0.30	31.49 ± 1.24	89.27 ± 0.75	84.08 ± 0.49
	(121, 7)‡	(115, 6)	(133, 4)	(176, 6)	(127, 5)
	-	p < 0.001	p < 0.001	p < 0.001	p < 0.001

Quantitation of spindle length (pole to pole distance), inter-kinetochore distance and kinetochore localisation of Bub1 and BubR1 in DLD-1 cells treated with GSK-3 inhibitors.

* Values in parentheses (Number of cells)

‡ Values in parentheses (Number of kinetochores, Number of cells)

§ Kruskal-Wallis Test (Nonparametric ANOVA), Dunn's Multiple Comparisons Test.

corresponding to the spindle midzone (Fig. 6B). In some cells, the peaks were further apart in drug-treated cells indicating an extended spindle length (Fig. 6B, top panel). However, in other cases there appeared to be little difference (6B, bottom panel). When we measured the pole-to-pole distance in control cells, the mean value was 8.4 ± 0.4 μm. The mean values derived from GSK-3 inhibitor-treated cells were marginally higher, reaching 10.4 ± 0.6 μm in the presence of AR-A014418 (Fig. 6C). However that these differences are not statistically significant (Table 4), possibly reflecting a small effect or our small sample size.

Tubulin intensity along the spindle length was, however, significantly different in drug-treated cells. In the examples shown in Figure 6B, the trough between the two peaks – which corresponds to the spindle midzone – is lower in both cases. Indeed, in control cells, the ratio of tubulin intensity at the midzone compared to the maximum value in that cells was 0.39 ± 0.02 (Fig. 6D, Table 4). By contrast, in drug-treated cells this value was reduced to between 0.21 ± 0.01 in the presence of SB-415286, and 0.26 ± 0.02 in the presence of CHIR99021. Thus, GSK-3 inhibitors do appear to affect spindle morphology.

GSK-3 inhibitors reduce Bub1 levels at aligned chromosomes

The spindle checkpoint maintains chromosome stability by delaying anaphase until all the chromosomes are correctly bioriented [49-51]. That cells treated with GSK-3 inhibitors delay mitosis in the presence of unaligned chromosomes indicates that the spindle checkpoint is largely intact (Fig. 3). Consistently, when exposed to the spindle toxins taxol and nocodazole, SB-415286 treated cells arrest in mitosis (data not shown). However, the spindle checkpoint is capable of delaying anaphase in response to a single unaligned chromosome [51,52]. Because drug-treated cells often enter anaphase with unaligned chromosomes (Fig. 3), it is possible that the GSK-3 inhibitors suppress the checkpoint signal below the threshold required to detect a single unaligned chromosome. While many factors determine spindle checkpoint signalling [53,54], kinetochore localisation of Bub1 and BubR1 is required for full checkpoint function [37,55]. Therefore, we analysed the levels of kinetochore bound Bub1 and BubR1 following drug exposure.

In control and drug-treated cells, Bub1 and BubR1 were recruited to kinetochores in prophase and prometaphase (not shown). In control cells, Bub1 and BubR1 persisted at metaphase kinetochores, albeit at reduced levels (Fig. 7A, B). In drug-treated cells, Bub1 and BubR1 were clearly present at the kinetochores of unaligned chromosomes. Consistent with our previous observations suggesting that Bub1 localisation is attachment-sensitive [36], Bub1 asymmetrically labelled the kinetochores of mono-oriented chromosomes, with the unattached kinetochore staining stronger (Fig. 7A, C). In addition, consistent with our previous notion that BubR1 localisation is tension-sensitive [36], BubR1 staining was more symmetrical at the kinetochores of mono-oriented chromosomes (Fig. 7B, C). Furthermore, pixel intensity-measurements revealed that the levels of Bub1 and BubR1 at these unaligned chromosomes were no different from unaligned kinetochores in control cells (data not shown). Thus, prior to chromosome alignment, the behaviour of Bub1

and BubR1 appear largely normal in the presence of the GSK-3 inhibitors.

The abundance of Bub1 and BubR1 at aligned chromosomes was however significantly reduced (Fig. 7A, B and Table 4). Pixel intensity-measurements showed that SB-415286, AR-A014418, 1-Azakenpaullone and CHIR99021 all reduced kinetochore bound Bub1, down to 25% in the case of AR-A014418 (Fig. 7E and Table 4). Kinetochore bound BubR1 was also reduced by all four drugs, most notably by SB-415286 and AR-A014418 (Fig. 7F and Table 4). One explanation for these observations is that the bioriented kinetochores had higher microtubule occupancy and/or were under more tension. To test this, we measured the inter-kinetochore distances of aligned chromosomes. In control cells, the mean inter-kinetochore distance was 0.91 ± 0.04 μm. In SB-415286- and AR-A014418-treated cells, this value increased to ~1.05 μm, a statistically significant difference (Fig 7D and Table 4). Although 1-Azakenpaullone and CHIR99021 had little effect, note that there is a correlation between inter-kinetochore distance and BubR1 levels. While SB-415286 and AR-A014418 increased inter-kinetochore distance and reduced BubR1, 1-Azakenpaullone and CHIR99021 had only modest effects on BubR1 binding and inter-kinetochore distance (Table 4). Significantly, SB-415286 and AR-A014418 also had more penetrant effects on chromosome alignment (Figs 2C, 3D) and pole-to-pole distance (Fig. 6C and Table 4).

GSK-3β RNAi induces mitotic defects

Our observations demonstrate that several different GSK-3 inhibitors effect spindle morphology and chromosome alignment, and elevate the chromosomes missegregation rate. Because we used a panel of structurally diverse compounds (Fig. 1), the simplest explanation is that the effects are due to inhibition of GSK-3. However, to rule out the possibility that the phenotypes observed may be due to off-target effects, we asked whether repression of GSK-3β by RNA interference yielded similar effects. We focussed on GSK-3β because this isoform localises to the mitotic spindle [33]. DLD-1 cells were transfected with siRNA duplexes designed to repress GSK-3β then immunoblotted with an antibody which recognises both GSK-3α and GSK-3β. Importantly, we observed a significant and selective reduction in GSK-3β levels (Fig. 8A). In the GSK-3β RNAi population, we frequently observed cells with micronuclei in the GSK-3β RNAi population (Fig. 8B), an indicator of chromosome missegregation [56]. Quantitation revealed that GSK-3β RNAi increased the number of cells with micronuclei by a factor of two 48-hours post transfection, and by almost 4-fold at 72 hours (Fig. 8C). Furthermore, we frequently observed metaphase spindles with multiple unaligned chromosomes (Fig. 8D). Quantitation showed a greater than 3-fold increase in such figures 72 hours after transfection (Fig. 8E). The spindle also appeared abnormal following GSK-3β RNAi, with an increase in astral microtubules (not shown) and an increase in spindle length; the mean pole-to-pole distance following repression of GSK-3β was 8.3 ± 0.4 μm compared to 7.7 ± 0.3 μm in control cells. Tubulin intensity at the spindle midzone was also significantly reduced ($p < 0.05$) following GSK-3β RNAi (Fig. 8F). BubR1 levels at metaphase kinetochores was significantly reduced; the mean BubR1/ACA ratio was 4.37 ± 0.94 in controls compared to 2.76 ± 0.24 in GSK-3β-deficient cells ($p < 0.05$). Inter-kinetochore distance was also significantly increased from 1.02 ± 0.03 μm in controls to 1.15 ± 0.04 μm following repression of GSK-3β ($p < 0.05$). Thus, as observed with the small molecule GSK-3 inhibitors, RNAi-mediated repression of GSK-3β affects spindle morphology, inhibits chromosome alignment and the fidelity of chromosome segregation.

Discussion

Small molecule GSK-3 inhibitors inhibit chromosome alignment

Here, we use small molecule inhibitors to probe GSK-3 function in cell cycle progression and mitotic chromosome segregation. Several inhibitors, including SB-415286, AR-A014418, 1-Azakenpaullone and CHIR99021, all significantly reduced phosphorylation of glycogen synthase in cells, indicating efficient cellular inhibition of GSK-3. Importantly, these four compounds inhibit chromosome alignment. Several other compounds, which reportedly inhibit GSK-3 *in vitro*, had little effect on glycogen synthase phosphorylation and had no effect on chromosome alignment. Why these latter inhibitors did not inhibit GSK-3 activity in cells is unclear but could be due to trivial reasons such as limited permeability. While the mode of action of these latter inhibitors is non-ATP competitive, the inhibitors which did inhibit GSK-3 activity in cells were all ATP competitors. This raises the possibility that their cellular effects may be due to inhibition of other protein kinases. However, all four inhibitors are relatively specific for GSK-3 inhibitors, at least *in vitro* [44,47,57,58]. Furthermore, they are all from different chemical classes and therefore likely to have different spectrums of "off-target" effects. Thus, the simplest explanation is that the chromosome alignment defect is due to inhibition of GSK-3. Indeed, the similarities between the GSK-3β RNAi phenotype and the inhibitor-induced phenotypes lends further weight to this notion. However, it will be important to test this hypothesis further in future studies, in particular the identification and characterisation of drug-resistant GSK3-β mutants will provide a powerful approach to dissecting the role of GSK-3 in cell cycle processes. In addition, analysing the effects these inhibitors have on GSK-3 null cells will help delineate off-target effects.

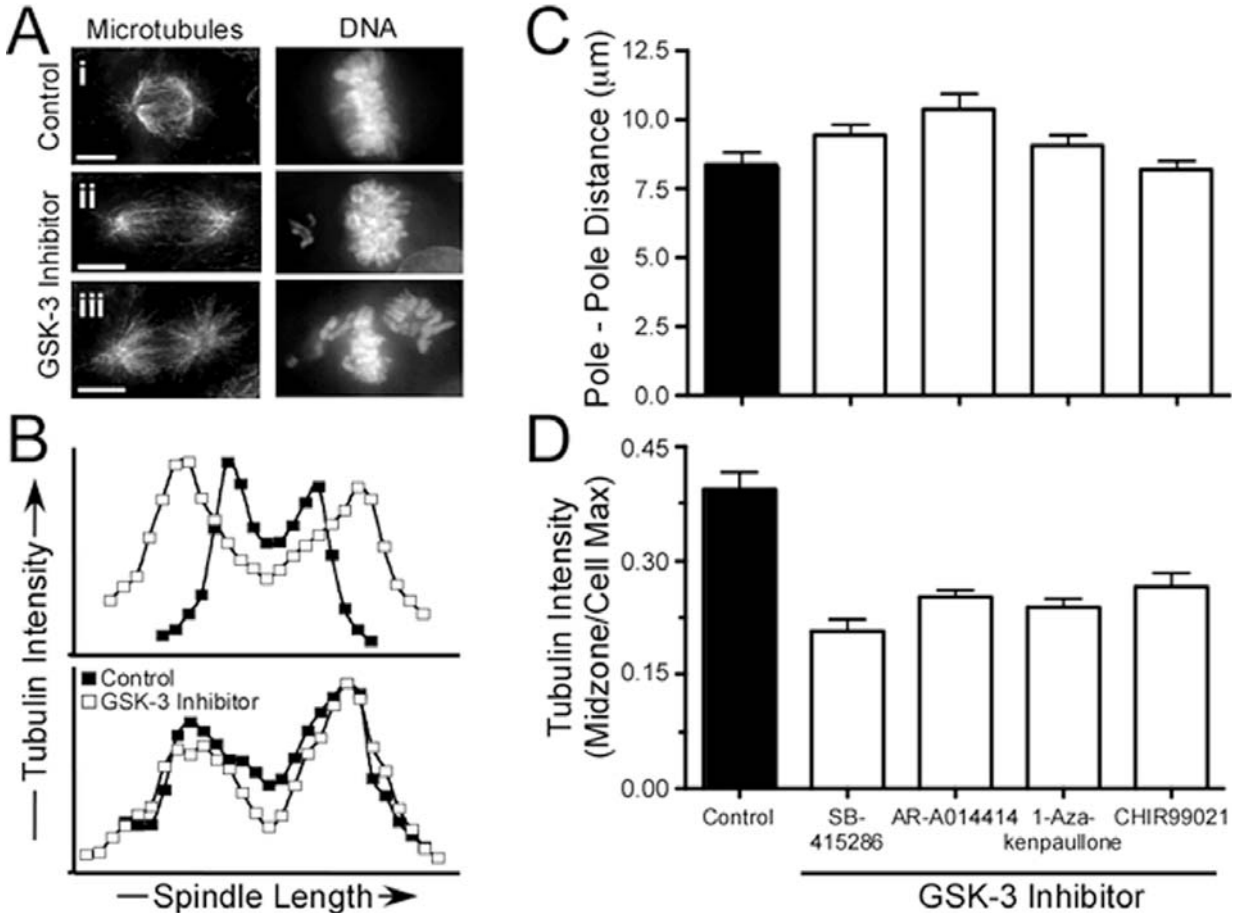

Figure 6

GSK-3 inhibitors weaken the spindle midzone. DLD-1 cells were incubated for 24 hours with GSK-3 inhibitors then fixed and stained to detect the microtubules and the chromosomes. (**A**) Projections of deconvolved image stacks showing representative mitotic spindles. Scale bar: 5 μm. (**B**) Graphs plotting tubulin intensity along the spindle axis. (**C**) Bar graphs plotting pole-pole distance. Values represent the mean and s.e.m. derived from at least 18 cells. (**D**) Bar graphs quantifying the tubulin intensity at the spindle midzone. Values represent the mean and s.e.m. derived from at least 15 cells. The cells in parts A-B were treated with either 2.5 μM 1-Azakenpaullone or 30 μM SB-415286

Regulation of GSK-3 at the spindle pole

The observation that phospho-GSK-3α/β (Ser21/9) localises to spindle poles in mitosis [33], raises the possibility that GSK-3 is somehow involved in regulating microtubule dynamics and/or spindle pole function. Indeed, Wakefield *et al* showed that cells treated with two GSK-3 inhibitors, SB-2 and SB-4 affected spindle assembly and inhibited chromosome alignment. Here, we have extended the observations of Wakefield *et al* by (*a*) using a panel of diverse GSK-3 inhibitors, (*b*) demonstrating that mitotic phenotypes correlate with GSK-3 inhibition and (*c*) further characterising the mitotic defects. In addition, we show that cells treated with GSK-3 inhibitors enter anaphase with unaligned chromosomes. Consistent with Wakefield *et al*, our observations indicate that spindle morphology was frequently abnormal in cells treated with GSK inhibitors, with elevated numbers of astral microtubules. Interestingly, *in vitro*, GSK-3 phosphorylates another centrosomal kinase, Aurora A, on serines 290/291[59]. This in turn results in Aurora A auto-phosphorylation on serine 349. When S290/291 and S349 were mutated to phospho-mimicing aspartates, Aurora A was less active towards CPEB, a substrate that becomes phosphorylated in *Xenopus* oocytes following progesterone stimulation [59]. This phosphorylation event results in the translation of mos and Cyclin B mRNAs, which in

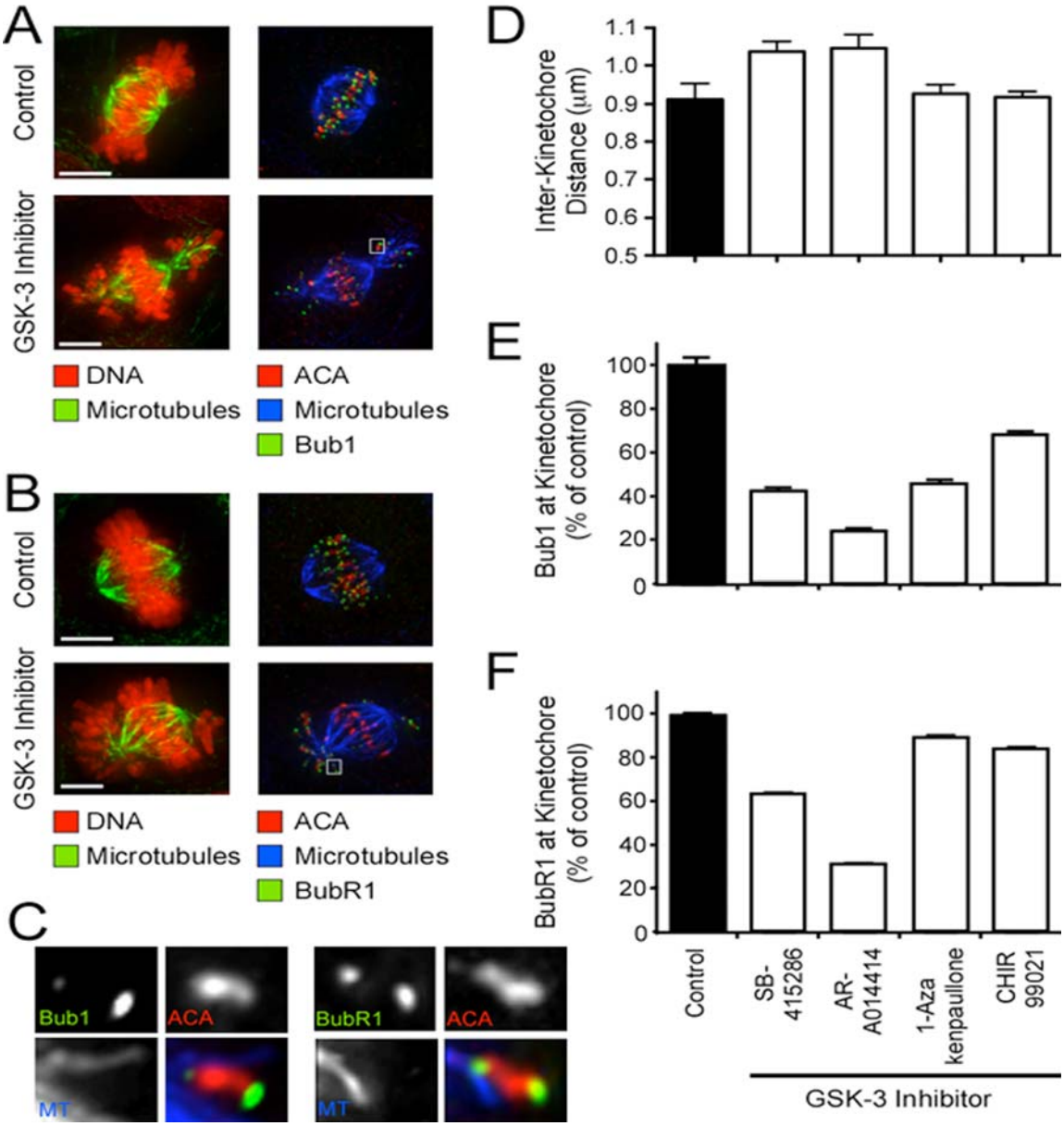

Figure 7

GSK-3 inhibitors increase inter-kinetochore distance. Drug-treated DLD-1 cells were fixed and stained to detect centromeres (ACA, red), kinetochores (Bub1 or BubR1, green), microtubules (green or blue) and the chromosomes (red) as indicated. (**A, B**) Projections of deconvolved image stacks showing reduced levels of Bub1 and BubR1 is at metaphase-kinetochores is reduced in GSK-3 inhibitor treated cells. Scale bars: 5 μm. (**C**) Projections of deconvolved image stacks showing the asymmetric labelling of Bub1 on the kinetochore of mono-orientated chromosomes. (**D**) Bar graph quantifying inter-kinetochore distance at metaphase chromosomes. Values represent the mean and s.e.m. derived from at least 20 kinetochores in at least 3 cells. (**E, F**) Bar graphs quantifying the levels of Bub1 and BubR1 at aligned chromosomes. Values represent the mean and s.e.m. derived from at least 64 kinetochores in at least 3 cells. The cells shown in (A) were treated with 30 μM SB-415286 and in (B) with 10 μM CHIR99021.

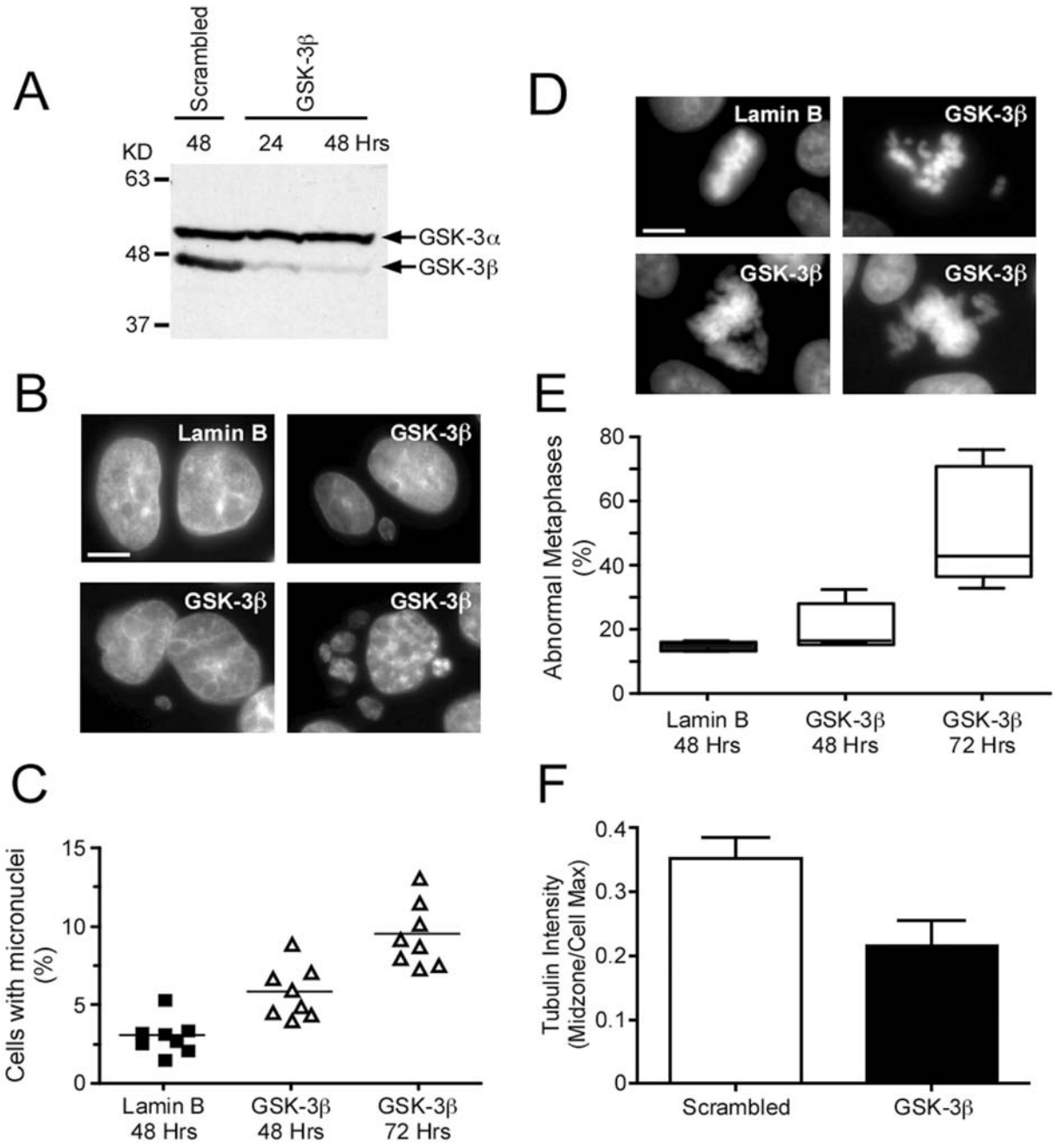

Figure 8

GSK-3β RNAi inhibits chromosome alignment. DLD-1 cells were transfected with siRNA duplexes designed to repress GSK-3β then analysed by immunoblot and immunofluorescence. (**A**) Immunoblot showing repression of GSK-3β. (**B**) Images of interphase cells showing micronuclei following repression of GSK3-β. (**C**) Scatter plot quantitating cells with micronuclei. The data is derived from four independent experiments, with each symbol representing an individual coverslip from which a minimum of 1,000 cells was counted. (**D**) Images of mitotic cells showing chromosome alignment defects in GSK-3β deficient cells. Bar = 5 μm. (**E**) Box plot quantitating abnormal metaphases in control (black bar) and GSK-3β RNAi (white bar) populations, 48 and 72 hours after transfection. The data is derived from three independent experiments. (F) Bar graphs quantifying the tubulin intensity at the spindle midzone. Values represent the mean and s.e.m. derived from at least 5 cells.

turn drives cell cycle progression. Conversely, an Aurora A harbouring non-phosphorylatable alanines at 290/291 and 349 was constitutively active towards CPEB. Thus, GSK-3 appears to negatively regulate Aurora A, at least in *Xenpous* oocyte maturation. Whether GSK-3 phosphorylates Aurora A in somatic cells remains to be seen, but evidence from several systems indicate that Aurora A is required for spindle assembly [60-62], and recently, we have shown that Aurora A kinase activity is required for spindle assembly in human cells [63]. Because GSK-3 is inactive when phosphorylated on serine 21/9, it is possible that downregulation of GSK-3 at the spindle poles allows localised Aurora A activation, which in turn modulates microtubule function thereby facilitating spindle assembly. Whether GSK-3 is active away from the centrosome in mitosis remains to be seen, but it is conceivable that drug-mediated inhibition of GSK-3 could result in activation of Aurora A elsewhere in the cell, not just at the spindle pole. This in turn may stabilise microtubules resulting in the excessive asters observed in drug-treated cells.

GSK-3, kinetochore – microtubule interactions and the spindle checkpoint

Cells treated with GSK-3 inhibitors align most of their chromosomes but have difficulty aligning them all and frequently enter anaphase with unaligned chromosomes. While the spindle defects may be sufficient to explain the chromosome misalignment, it is also possible that GSK-3 inhibition affects kinetochore behaviour. Support for this notion comes from the observation that the spindle checkpoint – which requires kinetochore function – is attenuated following GSK-3 inhibition. Clearly the spindle checkpoint is largely intact following GSK-3 inhibition: drug-treated cells delay anaphase onset in the presence of unaligned chromosomes (Fig. 4) and arrest when the spindle is destroyed with nocodazole (data not shown) However, drug-treated cells do enter anaphase with unaligned chromosomes, something which control cells never do. Furthermore, when HeLa cells were released from a G1/S block into SB-415286 plus nocodazole, the population mounted an attenuated checkpoint response, exhibiting a maximal mitotic index of ~40% (data not shown) compared to ~80% in controls (Fig. 3). Why the spindle checkpoint in GSK-3-inhibitor treated cells is attenuated remains to be seen: we did not observe any significant changes with respect to the levels of Bub1 and BubR1 at unaligned kinetochores (not shown). Interestingly however, levels of Bub1 and BubR1 were decreased at kinetochores of aligned chromosomes (Fig. 6). Because levels of kinetochore-bound Bub1 and BubR1 are indicators of microtubule occupancy and tension respectively [36], this suggests that GSK-3-inhibition actually promotes kinetochore – microtubule interactions. Consistently, inter-kinetochore distances increase in the presence of SB-415286 and AR-A014414. One possibility is that GSK-3-inhibition affects the spindle checkpoint via APC. Bub1 and BubR1 phosphorylate APC *in vitro*, an event which is enhanced if APC is already phosphorylated by GSK-3 [15]. Thus, following GSK-3 inhibition, phosphorylation of APC by Bub1 and BubR1 maybe attenuated.

Recently cells depleted of APC or expressing dominant negative mutants have been shown to have weakened collapsed spindles, defective kinetochore attachments, an increase in levels of kinetochore bound Bub1 and BubR1 and a decrease in tension across the kinetochore [16-18,21,64]. However, there appears to be no anaphase delay even though these cells go on and missegregate their chromosomes [65]. In contrast when GSK-3 is inhibited we observe an increase in spindle length and astral microtubules, a decrease in the level of kinetochore bound Bub1 and BubR1, an increase in the interkinetochore distance and a delay in chromosome alignment. This raises the possibility that GSK-3 negatively regulates APC's mitotic functions such that inhibiting GSK-3 activates APC, thereby yielding the opposite phenotype to APC depletion. Indeed inhibition of GSK-3 increases APC-microtubule interactions [13] which may help stabilise kinetochore-microtubule interactions.

Conclusion

GSK-3 and CIN

Our observations show that, at least in cultured cells, GSK-3 inhibitors induce chromosome non-disjunction, a phenotype that we also observed following RNAi-mediated repression of GSK-3β. Although GSK-3 inhibition affects spindle morphology, the chromosome alignment defect is the major contributing factor to non-disjunction. Is it possible that GSK-3 dysfunction causes chromosome instability in tumours? We feel that this is unlikely. Firstly, GSK-3 is rarely mutated in cancer [66]. Secondly, mouse knockouts are embryonic lethal [67]. Thus, in light of its essential and multi-faceted functions, GSK-3 dysfunction is likely to lead to cell death rather than provide a growth advantage. However, GSK-3 inhibitors are currently being investigated as potential therapeutics for a variety of chronic diseases such as diabetes and neurodegenerative disorders. Our observations suggest that GSK-3 inhibitors may have an unexpected consequence in these settings, namely the induction of chromosome instability, which may in turn promote tumourigenesis. Efforts to determine whether GSK-3 inhibitors induce chromosome instability in mouse models and patients seem to us to be imperative.

Methods

Cell culture and GSK-3 inhibitors

HeLa, HCT116, DLD-1 and DLD-1 cells stably expressing GFP-Histone H2B were all as described previously [38]. Cell culture conditions were as described [36]. Nocodazole (Sigma, 10 mg/ml in DMSO) was used at a final concentration of 0.2 μg/ml. The proteasome inhibitor MG132 (Calbiochem, 20 mM in DMSO) was used at a final concentration of 20 μM. RO-31-8220 (Calbiochem, 10 mM in DMSO) was used at a final concentration of 10 μM. SB-415286 (Tocris; 25 mM), TDZD-8 (Calbiochem; 20 mM), Inhibitor II (Calbiochem, 25 mM), OTDZT (Calbiochem; 31.8 mM), Inhibitor XI (Calbiochem; 25 mM), 1-Azakenpaullone (Calbiochem; 25 mM), AR-A014418 (Calbiochem, 25 mM), and CHIR99021 (kind gift from Philip Cohen; 10 mM) were dissolved in DMSO at the concentrations indicated, stored at -20°C in individual aliquots to avoid freeze thaw cycles, then freshly diluted in media. DMSO was added to control cultures to account for the solvent. Lithium Chloride (BDH) was dissolved in water at concentration of 1 M, filter sterilised and used at a final concentration of 40 mM.

Antibody Techniques

Immunoblotting was done as described previously [21,36] using the following antibodies: rabbit anti-phospho-glycogen synthase (Cell Signalling Tech, 1:1,000); mouse anti-glycogen synthase kinase 3 (4G-1E, Upstate, 1:500); mouse anti-phospho-nucleolin (TG3, kindly provided by Peter Davies, 1:25); sheep anti-Bub3 (SB3.2, 1:1000). Immunofluorescence was done as described [21] using the following antibodies: TAT-1, mouse anti-tubulin (1:100, ref. [68]); SBR1.1, sheep anti-BubR1 (1:1,000, ref [36]); SB1.3, sheep anti-Bub1 (1:1,000, ref [36]); ACA, human anti-centromere (kindly provided by Bill Earnshaw, 1:800). To analyse kinetochore – microtubule interactions and spindle morphology, cells were permeabilised for 90 seconds in a microtubule stabilising buffer (100 mM PIPES pH 6.8, 1 Mm MgCl, 0.1 Mm $CaCl_2$, 0.1% Triton X-100), fixed for 10 minutes in 4% formaldehyde, then blocked and incubated with the appropriate primary antibodies as described above. Following washes with PBST, cells were stained for 30 minutes at room temperature with the appropriate Cy2-, Cy3- or Cy5- conjugated secondary antibodies (Jackson Immuno-Research Laboratories), all diluted 1:500. Following washes, cells were stained with Hoechst 33358 at 1 μg/ml in PBST then mounted in 90% glycerol, 20 mM Tris-HCl pH 8.0. Deconvolution microscopy and pixel intensity quantitation was performed using a wide field optical sectioning microscope (Deltavision, Applied Precision) as described previously [36]. Briefly, for each cell, a Z-series of images at 0.2 μm intervals was captured at each wavelength and then processed using constrained iterative deconvolution. Deconvolved image stacks were projected and fluorescence signal intensities quantified using SoftWoRx (Applied Precision). To quantify the kinetochore bound protein, the average pixel intensities from at least 64 kinetochores from three or more cells was measured, background readings were subtracted and the values were then normalised against the ACA signal to account for any variations in staining or image acquisition. SoftWoRx was used to measure inter-kinetochore distance using Bub1 foci as indicated to determine kinetochore position. Tubulin intensity was determined as described previously [21,48]. Statistical analysis was performed using InStat®v3.0 (GraphPad Software Inc).

Cell biology

DNA content and mitotic index measurements and synchronisation of TA-HeLa cells at G1/S using double thymidine block were done as described previously [37], but using an FSE-conjugated MPM-2 antibody (Upstate Biotech). At least 10,000 cells were then analysed on a FACSCAN (Becton Dickson). For time-lapse analysis, DLD-1 cells expressing the GFP-Histone fusion protein were cultured on either individual 35 mm glass bottomed Petri dishes or 35 mm glass bottomed 6-well plates (MatTek Co). Microscopy was performed on a manual Axiovert 200 (Zeiss), equipped with a PZ-2000 automated stage (Applied Scientific Instrumentation) and an environmental control chamber (Solent Scientific), which maintained the cells at 37°C in a humidified stream of 5% CO_2, 95% air. Shutters, filter wheels and point visiting were driven by Metamorph software (Universal Imaging). Images were taken using a CoolSNAP HQ camera (Photometrics), while individual TIFF files were imported into Photoshop (Adobe) for printing or QuickTime (Apple) for movies. Nuclear envelope breakdown (NEB) was judged as the point when the prophase chromatin lost a smooth, linear periphery and the time of anaphase onset to be the first frame where coordinated pole wards movement was observed. Mitotic timing data is presented as box-and-whisker plots generated with Prism 4 (GraphPad), where the boxes show the median and interquartile range, while the whiskers show the entire range.

RNAi

siRNA duplexes (SMARTpool, Dharmacon Research) designed to repress GSK-3β or non-specific control pool duplexes or siRNA duplexes designed to target lamin B1were transfected into DLD-1 cells using OligofectAMINE™ (Invitrogen) as describe [69]. In brief, 4×10^4 cells were seeded in 24-well plates 24 hours prior to transfection in growth media without antibiotics. siRNA duplexes were mixed with OligofectAMINE™ in OptiMEM media without antibiotics and incubated for 20 minutes. siRNA/lipid complexes were then added to cells for 6 hours followed by addition of complete media containing 20% foetal calf serum. 24 hours later the cells were

replated onto coverslips or 6 well plates then analysed 24 hours later.

Authors' contributions

Project conceived and experiments designed by AT and SST. Experiments carried out by AT assisted by AR and OS. Manuscript prepared by AT and SST.

Acknowledgements

For generously providing reagents, we are indebted to Philip Cohen (Dundee), Peter Davies (New York) and Bill Earnshaw (Edinburgh). AT was funded by the Association for International Cancer Research. AR and OS were funded by studentships from the Wellcome Trust and the M.R.C. respectively. SST is a Cancer Research UK Senior Fellow.

References

1. Nicklas RB: **How cells get the right chromosomes.** *Science* 1997, **275:**632-637.
2. Chan GK, Liu ST, Yen TJ: **Kinetochore structure and function.** *Trends Cell Biol* 2005, **15:**589-598.
3. Cleveland DW, Mao Y, Sullivan KF: **Centromeres and kinetochores: from epigenetics to mitotic checkpoint signaling.** *Cell* 2003, **112:**407-421.
4. Maiato H, DeLuca J, Salmon ED, Earnshaw WC: **The dynamic kinetochore-microtubule interface.** *J Cell Sci* 2004, **117:**5461-5477.
5. Andrews PD, Knatko E, Moore WJ, Swedlow JR: **Mitotic mechanics: the auroras come into view.** *Curr Opin Cell Biol* 2003, **15:**672-683.
6. Pinsky BA, Biggins S: **The spindle checkpoint: tension versus attachment.** *Trends Cell Biol* 2005, **15:**486-493.
7. Kops GJ, Weaver BA, Cleveland DW: **On the road to cancer: aneuploidy and the mitotic checkpoint.** *Nat Rev Cancer* 2005, **5:**773-785.
8. Hanson CA, Miller JR: **Non-traditional roles for the Adenomatous Polyposis Coli (APC) tumor suppressor protein.** *Gene* 2005, **361:**1-12.
9. Nathke IS: **The adenomatous polyposis coli protein: the Achilles heel of the gut epithelium.** *Annu Rev Cell Dev Biol* 2004, **20:**337-366.
10. Bienz M: **The subcellular destinations of APC proteins.** *Nat Rev Mol Cell Biol* 2002, **3:**328-338.
11. Radtke F, Clevers H: **Self-renewal and cancer of the gut: two sides of a coin.** *Science* 2005, **307:**1904-1909.
12. Sieber OM, Tomlinson IP, Lamlum H: **The adenomatous polyposis coli (APC) tumour suppressor--genetics, function and disease.** *Mol Med Today* 2000, **6:**462-469.
13. Zumbrunn J, Kinoshita K, Hyman AA, Nathke IS: **Binding of the adenomatous polyposis coli protein to microtubules increases microtubule stability and is regulated by GSK3 beta phosphorylation.** *Curr Biol* 2001, **11:**44-49.
14. Fodde R, Kuipers J, Rosenberg C, Smits R, Kielman M, Gaspar C, van Es JH, Breukel C, Wiegant J, Giles RH, Clevers H: **Mutations in the APC tumour suppressor gene cause chromosomal instability.** *Nat Cell Biol* 2001, **3:**433-438.
15. Kaplan KB, Burds AA, Swedlow JR, Bekir SS, Sorger PK, Nathke IS: **A role for the Adenomatous Polyposis Coli protein in chromosome segregation.** *Nat Cell Biol* 2001, **3:**429-432.
16. Green RA, Kaplan KB: **Chromosome instability in colorectal tumor cells is associated with defects in microtubule plus-end attachments caused by a dominant mutation in APC.** *J Cell Biol* 2003, **163:**949-961.
17. Green RA, Wollman R, Kaplan KB: **APC and EB1 function together in mitosis to regulate spindle dynamics and chromosome alignment.** *Mol Biol Cell* 2005, **16:**4609-4622.
18. Dikovskaya D, Newton IP, Nathke IS: **The adenomatous polyposis coli protein is required for the formation of robust spindles formed in CSF Xenopus extracts.** *Mol Biol Cell* 2004, **15:**2978-2991.
19. Louie RK, Bahmanyar S, Siemers KA, Votin V, Chang P, Stearns T, Nelson WJ, Barth AI: **Adenomatous polyposis coli and EB1 localize in close proximity of the mother centriole and EB1 is a functional component of centrosomes.** *J Cell Sci* 2004, **117:**1117-1128.
20. Tighe A, Johnson VL, Albertella M, Taylor SS: **Aneuploid colon cancer cells have a robust spindle checkpoint.** *EMBO Rep* 2001, **2:**609-614.
21. Tighe A, Johnson VL, Taylor SS: **Truncating APC mutations have dominant effects on proliferation, spindle checkpoint control, survival and chromosome stability.** *J Cell Sci* 2004, **117:**6339-6353.
22. Yamashita YM, Jones DL, Fuller MT: **Orientation of asymmetric stem cell division by the APC tumor suppressor and centrosome.** *Science* 2003, **301:**1547-1550.
23. Rao CV, Yang YM, Swamy MV, Liu T, Fang Y, Mahmood R, Jhanwar-Uniyal M, Dai W: **Colonic tumorigenesis in BubR1+/-ApcMin/+ compound mutant mice is linked to premature separation of sister chromatids and enhanced genomic instability.** *Proc Natl Acad Sci U S A* 2005, **102:**4365-4370.
24. Tirnauer JS, Bierer BE: **EB1 proteins regulate microtubule dynamics, cell polarity, and chromosome stability.** *J Cell Biol* 2000, **149:**761-766.
25. Vaughan KT: **TIP maker and TIP marker; EB1 as a master controller of microtubule plus ends.** *J Cell Biol* 2005, **171:**197-200.
26. Su LK, Burrell M, Hill DE, Gyuris J, Brent R, Wiltshire R, Trent J, Vogelstein B, Kinzler KW: **APC binds to the novel protein EB1.** *Cancer Res* 1995, **55:**2972-2977.
27. Cohen P, Goedert M: **GSK3 inhibitors: development and therapeutic potential.** *Nat Rev Drug Discov* 2004, **3:**479-487.
28. Doble BW, Woodgett JR: **GSK-3: tricks of the trade for a multitasking kinase.** *J Cell Sci* 2003, **116:**1175-1186.
29. Jope RS, Johnson GV: **The glamour and gloom of glycogen synthase kinase-3.** *Trends Biochem Sci* 2004, **29:**95-102.
30. Morfini G, Szebenyi G, Brown H, Pant HC, Pigino G, DeBoer S, Beffert U, Brady ST: **A novel CDK5-dependent pathway for regulating GSK3 activity and kinesin-driven motility in neurons.** *Embo J* 2004, **23:**2235-2245.
31. Welcker M, Singer J, Loeb KR, Grim J, Bloecher A, Gurien-West M, Clurman BE, Roberts JM: **Multisite phosphorylation by Cdk2 and GSK3 controls cyclin E degradation.** *Mol Cell* 2003, **12:**381-392.
32. Ciani L, Krylova O, Smalley MJ, Dale TC, Salinas PC: **A divergent canonical WNT-signaling pathway regulates microtubule dynamics: dishevelled signals locally to stabilize microtubules.** *J Cell Biol* 2004, **164:**243-253.
33. Wakefield JG, Stephens DJ, Tavare JM: **A role for glycogen synthase kinase-3 in mitotic spindle dynamics and chromosome alignment.** *J Cell Sci* 2003, **116:**637-646.
34. Puziss JW, Hardy TA, Johnson RB, Roach PJ, Hieter P: **MDS1, a dosage suppressor of an mck1 mutant, encodes a putative yeast homolog of glycogen synthase kinase 3.** *Mol Cell Biol* 1994, **14:**831-839.
35. Goshima G, Iwasaki O, Obuse C, Yanagida M: **The role of Ppe1/PP6 phosphatase for equal chromosome segregation in fission yeast kinetochore.** *Embo J* 2003, **22:**2752-2763.
36. Taylor SS, Hussein D, Wang Y, Elderkin S, Morrow CJ: **Kinetochore localisation and phosphorylation of the mitotic checkpoint components Bub1 and BubR1 are differentially regulated by spindle events in human cells.** *J Cell Sci* 2001, **114:**4385-4395.
37. Taylor SS, McKeon F: **Kinetochore localization of murine Bub1 is required for normal mitotic timing and checkpoint response to spindle damage.** *Cell* 1997, **89:**727-735.
38. Morrow CJ, Tighe A, Johnson VL, Scott MI, Ditchfield C, Taylor SS: **Bub1 and aurora B cooperate to maintain BubR1-mediated inhibition of APC/CCdc20.** *J Cell Sci* 2005, **118:**3639-3652.
39. Cohen P, Frame S: **The renaissance of GSK3.** *Nat Rev Mol Cell Biol* 2001, **2:**769-776.
40. Parker PJ, Caudwell FB, Cohen P: **Glycogen synthase from rabbit skeletal muscle; effect of insulin on the state of phosphorylation of the seven phosphoserine residues in vivo.** *Eur J Biochem* 1983, **130:**227-234.
41. Klein PS, Melton DA: **A molecular mechanism for the effect of lithium on development.** *Proc Natl Acad Sci U S A* 1996, **93:**8455-8459.
42. Stambolic V, Ruel L, Woodgett JR: **Lithium inhibits glycogen synthase kinase-3 activity and mimics wingless signalling in intact cells.** *Curr Biol* 1996, **6:**1664-1668.

43. Potapova TA, Daum JR, Pittman BD, Hudson JR, Jones TN, Satinover DL, Stukenberg PT, Gorbsky GJ: **The reversibility of mitotic exit in vertebrate cells.** *Nature* 2006, **440:**954-958.
44. Coghlan MP, Culbert AA, Cross DA, Corcoran SL, Yates JW, Pearce NJ, Rausch OL, Murphy GJ, Carter PS, Roxbee Cox L, Mills D, Brown MJ, Haigh D, Ward RW, Smith DG, Murray KJ, Reith AD, Holder JC: **Selective small molecule inhibitors of glycogen synthase kinase-3 modulate glycogen metabolism and gene transcription.** *Chem Biol* 2000, **7:**793-803.
45. Lochhead PA, Coghlan M, Rice SQ, Sutherland C: **Inhibition of GSK-3 selectively reduces glucose-6-phosphatase and phosphatase and phosphoenolypyruvate carboxykinase gene expression.** *Diabetes* 2001, **50:**937-946.
46. Cline GW, Johnson K, Regittnig W, Perret P, Tozzo E, Xiao L, Damico C, Shulman GI: **Effects of a novel glycogen synthase kinase-3 inhibitor on insulin-stimulated glucose metabolism in Zucker diabetic fatty (fa/fa) rats.** *Diabetes* 2002, **51:**2903-2910.
47. Ring DB, Johnson KW, Henriksen EJ, Nuss JM, Goff D, Kinnick TR, Ma ST, Reeder JW, Samuels I, Slabiak T, Wagman AS, Hammond ME, Harrison SD: **Selective glycogen synthase kinase 3 inhibitors potentiate insulin activation of glucose transport and utilization in vitro and in vivo.** *Diabetes* 2003, **52:**588-595.
48. Holt SV, Vergnolle MA, Hussein D, Wozniak MJ, Allan VJ, Taylor SS: **Silencing Cenp-F weakens centromeric cohesion, prevents chromosome alignment and activates the spindle checkpoint.** *J Cell Sci* 2005, **118:**4889-4900.
49. Campbell MS, Gorbsky GJ: **Microinjection of mitotic cells with the 3F3/2 anti-phosphoepitope antibody delays the onset of anaphase.** *J Cell Biol* 1995, **129:**1195-1204.
50. Li X, Nicklas RB: **Mitotic forces control a cell-cycle checkpoint.** *Nature* 1995, **373:**630-632.
51. Rieder CL, Cole RW, Khodjakov A, Sluder G: **The checkpoint delaying anaphase in response to chromosome monoorientation is mediated by an inhibitory signal produced by unattached kinetochores.** *J Cell Biol* 1995, **130:**941-948.
52. Rieder CL, Schultz A, Cole R, Sluder G: **Anaphase onset in vertebrate somatic cells is controlled by a checkpoint that monitors sister kinetochore attachment to the spindle.** *J Cell Biol* 1994, **127:**1301-1310.
53. Musacchio A, Hardwick KG: **The spindle checkpoint: structural insights into dynamic signalling.** *Nat Rev Mol Cell Biol* 2002, **3:**731-741.
54. Taylor SS, Scott MI, Holland AJ: **The spindle checkpoint: a quality control mechanism which ensures accurate chromosome segregation.** *Chromosome Res* 2004, **12:**599-616.
55. Johnson VL, Scott MI, Holt SV, Hussein D, Taylor SS: **Bub1 is required for kinetochore localization of BubR1, Cenp-E, Cenp-F and Mad2, and chromosome congression.** *J Cell Sci* 2004, **117:**1577-1589.
56. Hoffelder DR, Luo L, Burke NA, Watkins SC, Gollin SM, Saunders WS: **Resolution of anaphase bridges in cancer cells.** *Chromosoma* 2004, **112:**389-397.
57. Kunick C, Lauenroth K, Leost M, Meijer L, Lemcke T: **1-Azakenpaullone is a selective inhibitor of glycogen synthase kinase-3 beta.** *Bioorg Med Chem Lett* 2004, **14:**413-416.
58. Bhat R, Xue Y, Berg S, Hellberg S, Ormo M, Nilsson Y, Radesater AC, Jerning E, Markgren PO, Borgegard T, Nylof M, Gimenez-Cassina A, Hernandez F, Lucas JJ, Diaz-Nido J, Avila J: **Structural insights and biological effects of glycogen synthase kinase 3-specific inhibitor AR-A014418.** *J Biol Chem* 2003, **278:**45937-45945.
59. Sarkissian M, Mendez R, Richter JD: **Progesterone and insulin stimulation of CPEB-dependent polyadenylation is regulated by Aurora A and glycogen synthase kinase-3.** *Genes Dev* 2004, **18:**48-61.
60. Roghi C, Giet R, Uzbekov R, Morin N, Chartrain I, Le Guellec R, Couturier A, Doree M, Philippe M, Prigent C: **The Xenopus protein kinase pEg2 associates with the centrosome in a cell cycle-dependent manner, binds to the spindle microtubules and is involved in bipolar mitotic spindle assembly.** *J Cell Sci* 1998, **111 (Pt 5):**557-572.
61. Garrett S, Auer K, Compton DA, Kapoor TM: **hTPX2 is required for normal spindle morphology and centrosome integrity during vertebrate cell division.** *Curr Biol* 2002, **12:**2055-2059.
62. Marumoto T, Honda S, Hara T, Nitta M, Hirota T, Kohmura E, Saya H: **Aurora-A kinase maintains the fidelity of early and late mitotic events in HeLa cells.** *J Biol Chem* 2003, **278:**51786-51795.
63. Girdler F, Gascoigne KE, Eyers PA, Hartmuth S, Crafter C, Foote KM, Keen NJ, Taylor SS: **Validating Aurora B as an anti-cancer drug target.** *J Cell Sci* 2006, **119:**3664-3675.
64. Dikovskaya D, Schiffmann D, Newton IP, Oakley A, Kroboth K, Sansom O, Jamieson TJ, Meniel V, Clarke A, Nathke IS: **Loss of APC induces polyploidy as a result of a combination of defects in mitosis and apoptosis.** *J Cell Biol* 2007, **176:**183-195.
65. Draviam VM, Shapiro I, Aldridge B, Sorger PK: **Misorientation and reduced stretching of aligned sister kinetochores promote chromosome missegregation in EB1- or APC-depleted cells.** *Embo J* 2006, **25:**2814-2827.
66. Sjoblom T, Jones S, Wood LD, Parsons DW, Lin J, Barber TD, Mandelker D, Leary RJ, Ptak J, Silliman N, Szabo S, Buckhaults P, Farrell C, Meeh P, Markowitz SD, Willis J, Dawson D, Willson JK, Gazdar AF, Hartigan J, Wu L, Liu C, Parmigiani G, Park BH, Bachman KE, Papadopoulos N, Vogelstein B, Kinzler KW, Velculescu VE: **The consensus coding sequences of human breast and colorectal cancers.** *Science* 2006, **314:**268-274.
67. Hoeflich KP, Luo J, Rubie EA, Tsao MS, Jin O, Woodgett JR: **Requirement for glycogen synthase kinase-3beta in cell survival and NF-kappaB activation.** *Nature* 2000, **406:**86-90.
68. Woods A, Baines AJ, Gull K: **A high molecular mass phosphoprotein defined by a novel monoclonal antibody is closely associated with the intermicrotubule cross bridges in the Trypanosoma brucei cytoskeleton.** *J Cell Sci* 1992, **103 (Pt 3):**665-675.
69. Ditchfield C, Johnson VL, Tighe A, Ellston R, Haworth C, Johnson T, Mortlock A, Keen N, Taylor SS: **Aurora B couples chromosome alignment with anaphase by targeting BubR1, Mad2, and Cenp-E to kinetochores.** *J Cell Biol* 2003, **161:**267-280.
70. Martinez A, Alonso M, Castro A, Perez C, Moreno FJ: **First non-ATP competitive glycogen synthase kinase 3 beta (GSK-3beta) inhibitors: thiadiazolidinones (TDZD) as potential drugs for the treatment of Alzheimer's disease.** *J Med Chem* 2002, **45:**1292-1299.
71. Naerum L, Norskov-Lauritsen L, Olesen PH: **Scaffold hopping and optimization towards libraries of glycogen synthase kinase-3 inhibitors.** *Bioorg Med Chem Lett* 2002, **12:**1525-1528.
72. O'Neill DJ, Shen L, Prouty C, Conway BR, Westover L, Xu JZ, Zhang HC, Maryanoff BE, Murray WV, Demarest KT, Kuo GH: **Design, synthesis, and biological evaluation of novel 7-azaindolyl-heteroaryl-maleimides as potent and selective glycogen synthase kinase-3beta (GSK-3beta) inhibitors.** *Bioorg Med Chem* 2004, **12:**3167-3185.